





# Contribution of Position a4S336 on Functional Expression and Up-regulation of a4b2 Neuronal Nicotinic Receptors

Gretchen Y. López-Hernández  Nilza M. Biaggi-Labiosa   
Alexis Torres-Cintrón  Alejandro Ortiz-Acevedo   
José A. Lasalde-Dominicci

Received: 20 February 2008 / Accepted: 20 June 2008  
Springer Science+Business Media, LLC 2008

**Abstract** Phosphorylation of the nicotinic acetylcholine receptor (nAChR) is believed to play a critical role in its nicotine-induced desensitization and up-regulation. We examined the contribution of a consensus PKC site in the M3/M4 intracellular loop (a4S336) on the desensitization and up-regulation of a4b2 nAChRs expressed in oocytes. Position a4S336 was replaced with either alanine to abolish potential phosphorylation at this site or with aspartic acid to mimic phosphorylation at this same site. Mutations a4S336A and a4S336D displayed a three-fold increase in the ACh-induced response and an increase in ACh EC<sub>50</sub>. Epibatidine binding revealed a three and sevenfold increase in surface expression for the a4S336A and a4S336D mutations, respectively, relative to wild-type, therefore, both mutations

enhanced expression of the a4b2 nAChR. Interestingly, the EC<sub>50</sub>'s and peak currents for nicotine activation remained unaffected in both mutants. Both mutations abolished the nicotine-induced up-regulation that is normally observed in the wild-type. The present data suggest that adding or removing a negative charge at this phosphorylation site cannot be explained by a simple straightforward on-and-off mechanism; rather a more complex mechanism(s) may govern the functional expression of the a4b2 nAChR. Along the same line, our data support the idea that phosphorylation at multiple consensus sites in the a4 subunit could play a remarkable role on the regulation of the functional expression of the a4b2 nAChR.

**Keywords** Whole-mount immunofluorescence assay Epibatidine binding Nicotine Voltage-clamp Confocal imaging

G. Y. López-Hernández  
Department of Pharmacology and Therapeutics,  
University of Florida, 100267, Gainesville,  
FL 32610-0267, USA

N. M. Biaggi-Labiosa J. A. Lasalde-Dominicci (✉)  
Department of Biology, University of Puerto Rico,  
JGD-114, 23360, San Juan, PR 00931-3360, USA  
e-mail: joseal@coqui.net; jlasalde@gmail.com

A. Torres-Cintrón  
Department of Chemistry and Chemical Biology,  
Cornell University, Ithaca, NY 14853, USA

A. Ortiz-Acevedo  
Department of Natural Sciences, University of Puerto  
Rico, 2500, Utuado, PR 00641-2500, USA

## Introduction

Chronic nicotine exposure induces an up-regulation of the a4b2 nicotinic acetylcholine receptors (nAChRs) in the CNS (Benwell et al. 1988; Breese et al. 1997; Flores et al. 1992; Marks et al. 1983; Schwartz and Kellar 1985; Whiteaker et al. 1998). Despite this increase in receptor number, chronic nicotine treatment produces loss in function as a result of their

rapid and persistent desensitization (Eilers et al. 1997; Ke et al. 1998; Lapchack et al. 1989; Lukas 1991). It is proposed that the property of desensitization of nAChRs is the driving force for the up-regulation (Fenster et al. 1999b; Marks et al. 1983; Schwartz and Kellar 1985).

Factors that regulate  $\alpha 4\beta 2$  nAChR desensitization may contribute to the long-term effects of nicotine on receptor number and function (Fenster et al. 1999a). One form of physiological regulation of nicotinic receptor desensitization is phosphorylation of nAChR subunits. Evidence for the role of phosphorylation on the desensitization process initially came from the study of muscle nAChRs; direct phosphorylation of  $\alpha$  and  $\beta$  subunits at serine residues by protein kinase A (PKA) increased the rate of desensitization (Huganir et al. 1986). Subsequently, studies of neuronal nicotinic receptors in chick sympathetic ganglia (containing  $\alpha 3$ ,  $\alpha 4$ ,  $\alpha 5$ ,  $\alpha 7$ ,  $\beta 2$ ,  $\beta 3$ , and  $\beta 4$  subunits) have indicated that cyclic AMP-dependent PKA and PKC can phosphorylate these receptors, and that exposure to phosphorylation may regulate agonist-induced desensitization (Downing and Roldan 1987; Vijayaraghavan et al. 1990).

The majority of the consensus phosphorylation sites are located in the cytoplasmic domain between M3 and M4 transmembrane regions (Swope et al. 1992). The  $\alpha 4$  subunit contains at least 13 putative phosphorylation consensus sites. Among them are the serine residues (S336, S364, S438, S469, S471, S490, S504, S516, and S589) that could be phosphorylated by PKC, PKA, and Casein kinase II. Two of the serine residues, S336 and S516, in the M3/M4 intracellular domain, are part of PKC phosphorylation consensus sites. Viseshakul et al. (1998) showed that the  $\alpha 4$  subunit of  $\alpha 4\beta 2$  nAChRs was phosphorylated in vivo. Furthermore, Wecker et al. (2001) demonstrated that the M3/M4 intracellular domain was phosphorylated by PKA and PKC.

Fenster et al. (1999a) provided compelling evidence suggesting that phosphorylation/dephosphorylation of S336 plays an important role in the modulation of nAChR desensitization as a result of short-term nicotine incubation. It is important to mention that Wecker et al. (2001) later referred this residue as S368 (numbered to include the signal peptide) and will be equivalent to S364 in our numbering. This residue is contained within the XRRXSX sequence that is phosphorylated by PKA (Wecker et al. 2001) and is different from the

residue mutated in this study, which is part of a putative consensus sequence phosphorylated by PKC (HHRSPRTHT) (Viseshakul et al. 1998).

In this study, we introduced alanine and aspartic acid residues at the S336 position. The replacement of serine by alanine was used to eliminate the PKC consensus site, whereas the introduction of aspartic acid should mimic a permanent phosphorylated state. We found that for both mutations the activation induced by ACh differ from the one induced by nicotine. Both  $\alpha 4S336A$  and  $\alpha 4S336D$  exhibited changes in ACh-induced macroscopic current and in the  $EC_{50}$  value for ACh, whereas there were no changes in these two properties when using nicotine as agonist. Given that the S336 position appears to be critical for the functional regulation of  $\alpha 4\beta 2$  nAChRs, it is reasonable to suggest that phosphorylation of several serine, threonine, or tyrosine residues on the  $\alpha 4$  and  $\beta 2$  M3/M4 cytoplasmic domains could play a major role in nAChR function during chronic nicotine exposure.

## Materials and Methods

### Site-directed Mutagenesis for the Generation of Mutant Neuronal $\alpha 4$ Subunits

The mutant  $\alpha 4$  subunits were created using QuikChange site-directed mutagenesis kit (Stratagene, La Jolla, CA). pGEMHE vector with *Rattus norvegicus* cDNA coding for  $\alpha 4$  neuronal nAChR subunit was used as DNA template in the PCR reaction. The oligonucleotide primers containing the desired mutation (Life Technologies-Gibco BRL, Gaithersburg, MD), each complementary to opposite strands of the vector, were extended during temperature cycling by the polymerase. The reaction mixture contains 5  $\mu$ l of 10 $\times$  reaction buffer, 50 ng of DNA template, 125 ng of each oligonucleotide primers, 1  $\mu$ l of dNTP mix, 1  $\mu$ l (2.5 units) of *Pfu Turbo* polymerase and water to a final volume of 50  $\mu$ l. The cycling parameters consisted of 16 cycles of plasmid denaturation for 30 s at 95C, primers annealing for 1 min at 55C, and extension for 10.20 min at 68C. Incorporation of the oligonucleotide primers generates a mutated plasmid containing staggered nicks. After DNA amplification the samples were digested with *Dpn I* endonuclease in order to digest the parental DNA

template and to select for mutation-containing synthesized DNA. The nicked vector DNA containing the desired mutation was transformed into *Escherichia coli* XL1-Blue supercompetent cells. The DNA was purified using QIAprep spin miniprep kit (Quiagen, Germantown, MD) and then sequenced.

#### In vitro Synthesis of mRNA and Oocyte Microinjection

Subunit mRNA was synthesized in vitro from linearized pGEMHE plasmid templates of *A. norvegicus* cDNA coding for  $\alpha 4$  and  $\beta 2$  nAChR subunits using the mMessage mMachine RNA transcription kit (Ambion, Austin, TX). mRNA mixtures of  $\alpha 4$  and  $\beta 2$  subunits were prepared at a 2:3  $\mu\text{g}$  ratio. The mRNA mixture was microinjected, using a displacement injector (Drummond Instruments, Broomhall, PA), into stages V and VI oocytes that had been extracted, incubated in collagenase Type 1A (Sigma, St. Louis, MO) and defolliculated by manual dissection. The injected oocytes were incubated at 20°C for 3 days in 0.5 $\times$  Leibovitz's L-15 medium (Invitrogen) supplemented with 400  $\mu\text{g}/\text{ml}$  bovine serum albumin, 119 mg/ml penicillin, 200 mg/ml streptomycin, and 110 mg/ml pyruvic acid. Electrophysiological experiments were performed after the third day of mRNA injection.

#### Electrophysiological Characterization of $\alpha 4\beta 2$ nAChRs

Oocytes injected with the mRNA transcripts of  $\alpha 4$  and  $\beta 2$  subunits were characterized using two-electrode voltage clamp. ACh- and nicotine-induced currents were recorded at 20°C, 3 days after mRNA injection, with a GeneClamp 500B Amplifier (Axon Instruments, Foster City, CA). Electrodes were filled with 3 M KCl and had a resistance of less than 2 M $\Omega$ . Impaled oocytes in the recording chamber were continuously perfused at a rate of 0.75 ml/s with MOR2 buffer (115 mM NaCl, 2.5 mM KCl, 5 mM HEPES, 1 mM  $\text{Na}_2\text{HPO}_4$ , 0.2 mM  $\text{CaCl}_2$ , 5 mM  $\text{MgCl}_2$ , and 0.5 mM EGTA, pH 7.4). All the reagents used were purchased from Sigma-Aldrich, Co. (St. Louis, MO). For dose-response curves, each oocyte was held at a membrane potential of  $-70$  mV. Membrane currents were digitized using the DigiData 1200 interface (Axon Instruments, CA), filtered at

2 kHz during recording. The Whole Cell Program 2.3 (provided by Dr. J. Dempster, University of Strathclyde, UK) running on a Pentium III-based computer was used for data acquisition. Data analysis was performed using Prism 3.0 (Graphpad Software, San Diego, CA). Dose-response data for the  $\alpha 4\beta 2$  combination were collected using nine ACh doses (0.1, 0.3, 1, 3, 10, 30, 100, 300, and 3,000  $\mu\text{M}$ ) or seven nicotine concentrations (0.1, 1, 3, 10, 30, 100, and 300  $\mu\text{M}$ ). The data were fitted using one- and two-component sigmoidal dose-response equations,  $Y = I/I_{\text{maxBottom}} + (I/I_{\text{maxTop}} - I/I_{\text{maxBottom}})/(1 + 10^{((\text{LogEC}_{50} - X) \times \text{HillSlope}))}$  and  $Y = I/I_{\text{maxBottom}} + [(I/I_{\text{maxTop}} - I/I_{\text{maxBottom}}) \times \text{Fraction}/(1 + 10^{((\text{LogEC}_{50,1} - X) \times \text{HillSlope}_{.1}))}] + [(I/I_{\text{maxTop}} - I/I_{\text{maxBottom}}) \times (1 - \text{Fraction})/(1 + 10^{((\text{LogEC}_{50,2} - X) \times \text{HillSlope}_{.2}))}]$ , respectively, where  $X$  is the logarithm of concentration and  $Y$  is the response. Additionally, four consecutive pulses of 300  $\mu\text{M}$  ACh or 30  $\mu\text{M}$  nicotine were applied to each oocyte and the nAChR macroscopic responses were recorded. Between each agonist application the oocyte was washed with MOR2 buffer for 5 min. In order to evaluate recovery, after the consecutive ACh or nicotine pulses, oocytes were washed with MOR2 buffer for 20 min and the agonist-induced macroscopic currents were measured. The protocol followed in the experiments involving acute nicotine exposure consisted of measuring the current induced by four consecutive applications of 300  $\mu\text{M}$  ACh. Between each ACh application, the oocyte was washed with 1.0  $\mu\text{M}$  nicotine-containing MOR2 for 5 min. That is, a total of three washes for the four ACh applications. We chose 300  $\mu\text{M}$  ACh based on the maximal response observed for  $\alpha 4\beta 2$  nAChRs using this ACh concentration. In order to calculate percent recovery, oocytes were washed for 20 min with nicotine-free MOR2 buffer after the last nicotine wash. We also conducted experiments to assess the effect of chronic nicotine exposure on the ACh-induced responses for wild-type and mutant  $\alpha 4\beta 2$  nAChRs. To that end, we obtained ACh dose-response curves (0.1, 0.3, 1, 3, 10, 30, 100, 300, and 3,000  $\mu\text{M}$ ) before and after prolonged nicotine incubation. For this nicotine incubation, oocytes were placed in L-15 medium supplemented with nicotine at a final concentration of 1  $\mu\text{M}$  for 24 h. Subsequently, oocytes were washed for 6 min by perfusing with MOR2 buffer. Finally, ACh dose-responses were determined as were done

prior to the chronic nicotine incubation. The peak currents at 300  $\mu$ M ACh were measured before and after 1  $\mu$ M nicotine exposure. Data are expressed as mean  $\pm$  SEM. One-way ANOVA was performed using Prism 3.0 (Graphpad Software, San Diego, CA). Results were compared with two-tailed Student's *t*-test using Graphpad Prism 3.0.

#### Immunofluorescence Assay for $\alpha$ 4 $\beta$ 2 Neuronal nAChR

*Xenopus* oocytes were injected with the mRNA transcripts of  $\alpha$ 4 and  $\beta$ 2 in subunit ratio of 2:3. Oocytes were incubated 72 h (3 days) in L-15 medium supplemented with antibiotics and antimycotics. On the third day of injection, 300  $\mu$ M ACh-induced currents were measured using the two-electrode voltage clamp technique. Oocytes to be compared were paired according to their similar current profile, i.e., with not more than 400 nA difference. Nicotine pre-incubation consisted of 24 h in L-15 medium supplemented with 1.0  $\mu$ M nicotine. Non-incubated oocytes were placed on L-15 nicotine-free solution. Following chronic exposure to nicotine, incubated and non-incubated oocytes were dehydrated with 1:1 Me<sub>2</sub>SO:methanol solution mixture, rehydrated with MOR2 buffer without EGTA (115 mM NaCl, 2.5 mM KCl, 5 mM HEPES, 1 mM NaH<sub>2</sub>PO<sub>4</sub>, 0.2 mM CaCl<sub>2</sub>, and 5 mM MgCl<sub>2</sub>, pH 7.4), and then fixed in 4% paraformaldehyde. Oocytes were then incubated in goat serum blocking solution prior to antibody treatment. They were then incubated overnight with a monoclonal antibody against the extracellular domain of the  $\alpha$ 4 nAChR subunit (mAb299, purchased from Covance Co.), and then washed with MOR2 solution. Finally, oocytes were incubated overnight with a secondary antibody conjugated to fluorescein isothiocyanate (Kirkegaard and Perry Laboratories, Inc., Gaithersburg, MD). Goat serum and antibodies were diluted in MOR2 buffer supplemented with 0.1% Triton X-100.

All images were acquired using a Zeiss LSM 510 confocal microscope (Carl Zeiss, Inc., Thornwood, NY) equipped with a Plan-Neofluar 100/0.3 objective. Multiple images (optical slices; 5  $\mu$ m thick) were acquired to construct Z stacks from each oocyte. Pinhole size, photomultiplier gain and offset, pixel size, and data depth settings were kept the same for all the images acquired in each experiment.

Auto fluorescence and background noise intensity values were obtained from non-injected oocytes in each experiment. We used MetaMorph (Universal Imaging Corporation, Downingtown, PA) to process each image. The threshold function was used to eliminate the fluorescence intensity values from pixels not contributing to the image (e.g., background and auto fluorescence). In addition, the same area ( $\mu$ m<sup>2</sup>) was selected for each control–experimental pair analyzed in order to make comparisons between optical slices. The total fluorescence intensity value was then calculated from each optical slice from the control and nicotine-incubated oocyte.

#### Epibatidine Binding Assay

[<sup>125</sup>I]-epibatidine (PerkinElmer Life Sciences, Boston, MA) binding assays were performed to determine membrane expression of nAChR in oocytes. The oocytes were incubated in 50 pM [<sup>125</sup>I]-epibatidine with 5 mg/ml albumin serum bovine in MOR2 without EGTA at room temperature for 2 h. Non-injected oocytes were also incubated with [<sup>125</sup>I]-epibatidine to measure non-specific binding (Beckman Gamma 5500). Excess epibatidine was removed by washing each oocyte with 60 ml of MOR2 without EGTA. A standard linear regression was obtained by plotting the counts per minute against [<sup>125</sup>I]-epibatidine concentration (0.5–20 fmol).

## Results

### Functional Properties and Expression of $\alpha$ 4 $\beta$ 2 Mutant nAChRs

The functional effects of substitution of a serine residue at position 336 of the  $\alpha$ 4 subunit on the activation properties of  $\alpha$ 4 $\beta$ 2 nAChR were evaluated using two-electrode voltage clamp recording. We measured the current response to several concentrations of ACh and nicotine. The average ACh- and nicotine-induced macroscopic peak currents are shown in Fig. 1c. The  $\alpha$ 4S336 mutants displayed a significant threefold increase in the ACh-induced macroscopic peak current (Fig. 1c) compared to the wild-type receptor. There was no significant difference in the nicotine-induced macroscopic peak

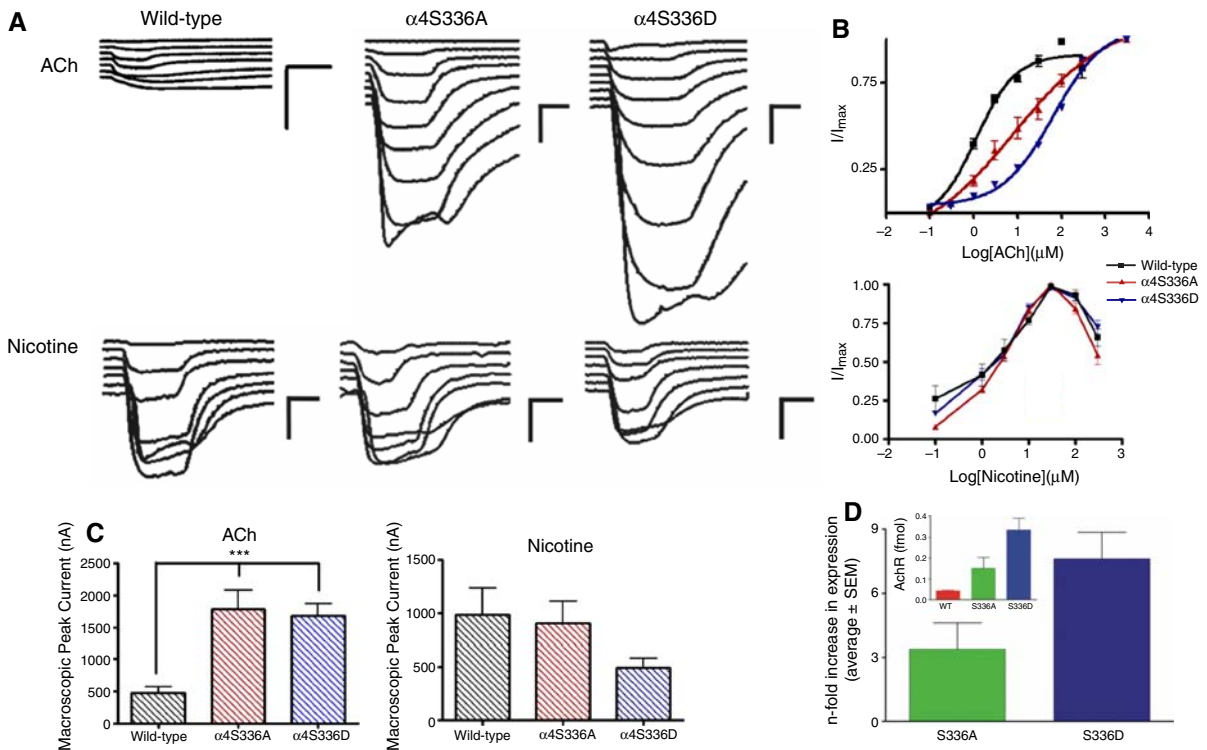


**Fig. 1** Effects of mutations at residue S336 of the  $\alpha 4b2$  nAChR subunit in the functional properties of  $\alpha 4b2$  nAChRs. Voltage clamp recording was used to determine the macroscopic response of wild-type and mutant  $\alpha 4b2$  nAChRs to several ACh or nicotine concentrations. **a)** Family of ACh- and nicotine-induced macroscopic currents recorded from *Xenopus* oocytes expressing wild-type,  $\alpha 4S336A$ , and  $\alpha 4S336D$   $\alpha 4b2$  nAChRs. Calibration bars are shown at the right of each current family, 500 nA (vertical bars) and 8 s (horizontal bars). **(b)** Dose-response relationships using ACh and nicotine as agonists for wild-type (black),  $\alpha 4S336A$  (red), and  $\alpha 4S336D$  (blue)  $\alpha 4b2$  receptors. ACh dose-response curves for mutants were determined using nine concentrations (0.1, 0.3, 1, 3, 10, 30, 100, 300, and 300  $\mu M$ ), whereas seven ACh concentrations (0.1, 1, 3, 10, 30, 100, and 300  $\mu M$ ) were tested to characterize wild-type receptor. Nicotine dose-response relationships were obtained from seven agonist concentrations (0.1, 1, 3, 10, 30, 100, and 300  $\mu M$ ). Agonist-induced responses were normalized to the maximum response ( $I/I_{max}$ ). ACh dose-response curves were fitted using a single Hill equation and a two-component Hill equation. A better fit ( $R^2 = 0.995$ ) was obtained using the two-component equation for the  $\alpha 4S336D$  mutant (Figs. 1b and 3b). The estimated ACh  $EC_{50}$  values for the  $\alpha 4S336D$  mutant receptor were  $17.4 \pm 1.4$  and  $137.7 \pm 0.1 \mu M$  (Table 1). The  $EC_{50}$  values for ACh activation of wild-type and  $\alpha 4S336A$  mutant receptors were  $1.1 \pm 0.1$  and  $8.6 \pm 0.2 \mu M$ , respectively (Table 1). Statistical analysis using unpaired *t*-test showed significant difference in the ACh  $EC_{50}$  values between wild-type and  $\alpha 4S336A$  mutants ( $P < 0.05$ ). The dose-response curves for nicotine showed a bell-shaped profile for the three  $\alpha 4b2$  nAChR subtypes studied (Fig. 1b). No significant difference was observed in the nicotine  $EC_{50}$  values among the three  $\alpha 4b2$  nAChR subtypes (Table 1). **(c)** Bar graphs illustrating ACh- or nicotine-induced peak current for wild-type,  $\alpha 4S336A$ , and  $\alpha 4S336D$   $\alpha 4b2$  nAChRs. The peak currents were obtained at 300  $\mu M$  ACh and 30  $\mu M$  nicotine. Statistical analysis was performed using one-way ANOVA with Dunnett's multiple comparison test ( $***P < 0.01$ ). **(d)** Bar graphs illustrating a summary of the results of the [<sup>3</sup>H]-epibatidine binding assays. Insert illustrates the expression values in fmols for wild-type ( $n = 3$ ; red),  $\alpha 4S336A$  ( $n = 6$ ; green), and  $\alpha 4S336D$  ( $n = 7$ ; blue). The main bar graph illustrates the fold increase (mutant expression divided by wild-type expression) in expression for the  $\alpha 4S336A$  (green) and  $\alpha 4S336D$  (blue) mutants. Values are presented as mean  $\pm$  SEM.

current among the  $\alpha 4b2$  nAChRs studied (Fig. 1c). The corresponding dose-response curves for ACh and nicotine are shown in Fig. 1b. ACh dose-response curves were fitted using a single Hill equation and a two-component Hill equation. A better fit ( $R^2 = 0.995$ ) was obtained using the two-component equation for the  $\alpha 4S336D$  mutant (Figs. 1b and 3b). The estimated ACh  $EC_{50}$  values for the  $\alpha 4S336D$  mutant receptor were  $17.4 \pm 1.4$

and  $137.7 \pm 0.1 \mu M$  (Table 1). The  $EC_{50}$  values for ACh activation of wild-type and  $\alpha 4S336A$  mutant receptors were  $1.1 \pm 0.1$  and  $8.6 \pm 0.2 \mu M$ , respectively (Table 1). Statistical analysis using unpaired *t*-test showed significant difference in the ACh  $EC_{50}$  values between wild-type and  $\alpha 4S336A$  mutants ( $P < 0.05$ ). The dose-response curves for nicotine showed a bell-shaped profile for the three  $\alpha 4b2$  nAChR subtypes studied (Fig. 1b). No significant

Table 1 Effects of mutations  $\alpha 4\beta 2$  S336 in the functional properties of  $\alpha 4\beta 2$  nAChRs expressed in *Xenopus* oocytes

AChR type ( $\alpha 4\beta 2$ )	ACh			Nicotine		
	EC <sub>50</sub> ± SEM (μM)	Hill coefficient	<i>n</i>	EC <sub>50</sub> ± SEM (μM)	Hill coefficient	<i>n</i>
Wild-type	1.1 ± 0.1	0.97 ± 0.1	9	2.5 ± 0.1	1.6 ± 0.7	7
$\alpha 4\beta 2$ S336A	8.6 ± 0.2*	0.4 ± 0.1*	9	1.8 ± 0.1	1.7 ± 0.6	5
$\alpha 4\beta 2$ S336D	17.4 ± 1.4*	0.6 ± 0.4*	5	2.0 ± 0.1	1.4 ± 0.3	13
	137.7 ± 0.1*	2.2 ± 2.7*				

Values are given as the mean ± SEM. \* Indicates  $P < 0.05$ , *n* indicates the number of oocytes tested

difference was found among the mean nicotine EC<sub>50</sub> and Hill slope values for the mutant and wild-type receptors (Table 1).

The increase in macroscopic peak current induced by the  $\alpha 4\beta 2$  S336 mutants (Fig. 1c) suggests that these mutations result in an increase in nAChR expression. [125I]-epibatidine assays were thus performed to determine membrane nAChR expression for wild-type and the  $\alpha 4\beta 2$  S336 mutants (Fig. 1d). The calculated expressions (fmol) for wild-type,  $\alpha 4\beta 2$  S336A and  $\alpha 4\beta 2$  S336D, were 0.04 ± 0.003, 0.15 ± 0.05, and 0.33 ± 0.05 (Fig. 1d, insert). These numbers correspond to an *m*-fold increase in expression, relative to that of wild-type, of 3.40 ± 1.21 and 7.61 ± 1.25 for the  $\alpha 4\beta 2$  S336A and  $\alpha 4\beta 2$  S336D mutants, respectively (Fig. 1d).

#### Desensitization of $\alpha 4\beta 2$ Mutant Receptors

Figure 2 illustrates the effect of consecutive applications of 300 μM ACh and 30 μM nicotine in the macroscopic response of mutant receptors. Consecutive ACh applications produced only a mild current loss in the mutant and wild-type  $\alpha 4\beta 2$  receptors (Fig. 2c). The percentages of current lost from their original macroscopic current after repetitive pulses of 300 μM ACh were 19 ± 4, 18 ± 3, and 6 ± 3 for wild-type,  $\alpha 4\beta 2$  S336A, and  $\alpha 4\beta 2$  S336D, respectively. The  $\alpha 4\beta 2$  S336D mutant exhibited the lowest loss of macroscopic current as result of consecutive applications of ACh (Fig. 2b, c). This lower percent of current lost for  $\alpha 4\beta 2$  S336D was significantly different from the wild-type receptor (Fig. 2c). The mutants and wild-type receptor displayed an increase in the progressive loss of macroscopic current after consecutive applications of 30 μM nicotine. The percentages of current loss were 51 ± 4 for wild-type, 68 ± 3 for  $\alpha 4\beta 2$  S336A, and 59 ± 2 for  $\alpha 4\beta 2$  S336D (Fig. 2c). The mean current

loss after consecutive applications of nicotine was significantly different between  $\alpha 4\beta 2$  S336A mutant and wild-type ( $P < 0.01$ ). Also acute nicotine exposure experiments were performed in which 1 μM nicotine was acutely applied between ACh applications as described under section "Materials and methods" (Fig. 2). The percentages of current lost from their original macroscopic current after acute nicotine exposure were 7 ± 2, 68 ± 7, and 60 ± 11 for wild-type,  $\alpha 4\beta 2$  S336A, and  $\alpha 4\beta 2$  S336D, respectively. The mean current loss after acute nicotine exposure was not significantly different.

The amount of recovery was measured (see section "Materials and methods") for each experimental condition tested (Fig. 2d). After consecutive applications of 300 μM ACh all three subtypes recovered a considerable amount of their initial current, 85 ± 6% for wild-type, 89 ± 6% for  $\alpha 4\beta 2$  S336A, and 94 ± 4% for  $\alpha 4\beta 2$  S336D. The means of the amount of current recovered after consecutive applications of ACh were not significantly different. In contrast, after repetitive pulses of 30 μM nicotine the mutant receptors recovered <50% of their initial current. The percentages of current recovered were 54 ± 4, 30 ± 3, and 38 ± 3 for wild-type,  $\alpha 4\beta 2$  S336A, and  $\alpha 4\beta 2$  S336D, respectively. The mean values of the recovered current after consecutive application of 30 μM nicotine of both mutants were significantly different from wild-type  $\alpha 4\beta 2$  nAChR ( $P < 0.01$ ). After acute exposure to 1 μM nicotine, the percentages of current recovered were 43 ± 3, 61 ± 7, and 61 ± 8 for wild-type,  $\alpha 4\beta 2$  S336A, and  $\alpha 4\beta 2$  S336D, respectively.

#### Chronic Nicotine Exposure and Activation of Mutant $\alpha 4\beta 2$ nAChRs

In order to evaluate the effect of chronic nicotine exposure on the functional activation of oocytes

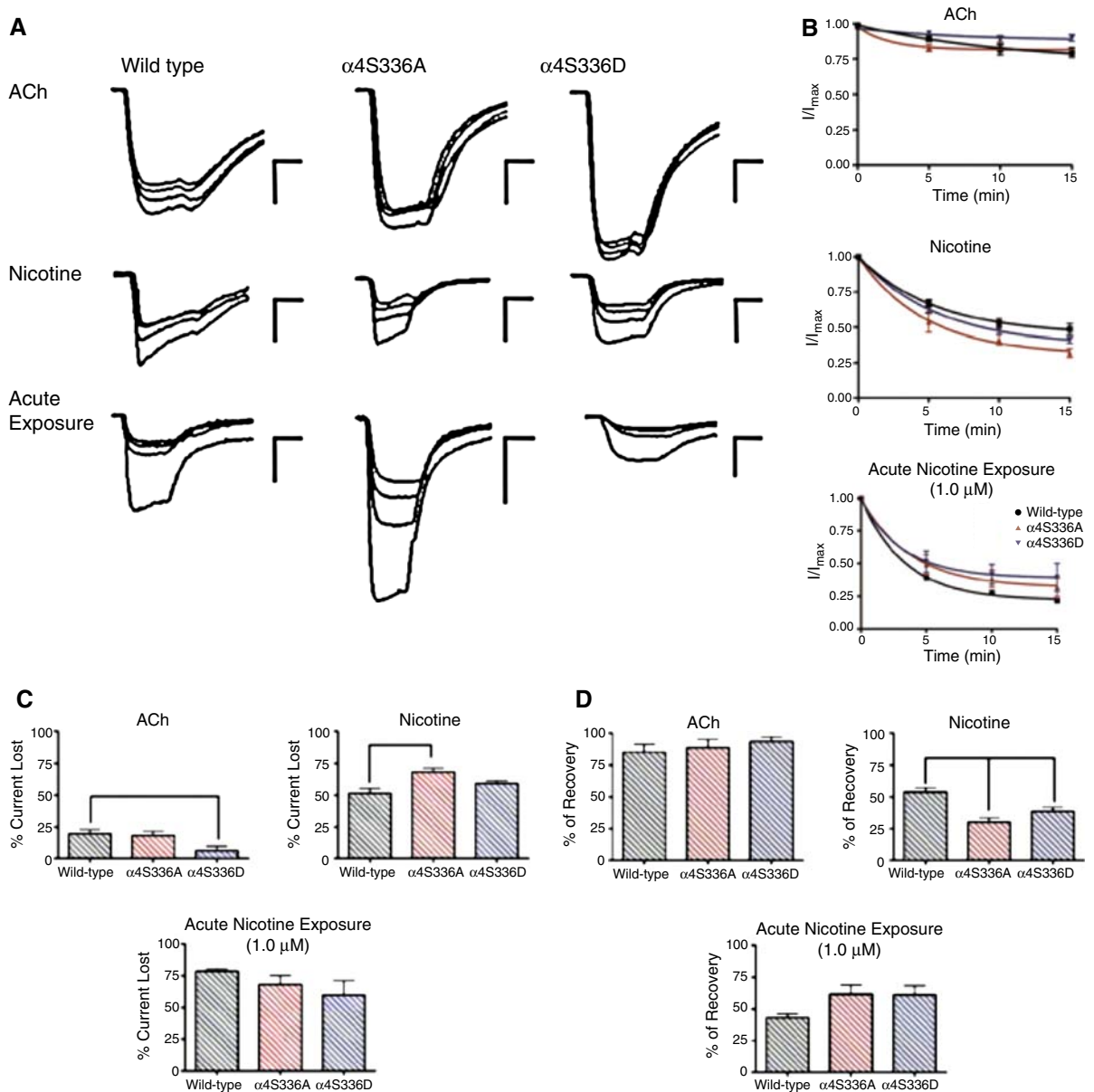


**Fig. 2** ACh- and nicotine-induced desensitization of mutant  $\alpha 4\beta 2$  nAChRs. **(a)** Family of current traces for wild-type,  $\alpha 4S336A$ , and  $\alpha 4S336D$   $\alpha 4\beta 2$  nAChRs representing the response to consecutive applications of agonist. The macroscopic responses to four consecutive applications of  $100 \mu M$  ACh or  $30 \mu M$  nicotine were recorded for each  $\alpha 4\beta 2$  subtype tested. Oocytes were washed with MOR2 buffer between each agonist pulse for 5 min (a total of three washes for four agonist applications). The protocol of acute nicotine exposure experiment consisted of measuring the current induced by four consecutive applications of  $30 \mu M$  ACh. Between each ACh application, the oocyte was washed with  $1 \mu M$  nicotine-containing MOR2 for 5 min. Calibration bars are shown at the right of each current family, 500 nA (vertical bars) and 8 s (horizontal bars). **(b)** Graphs illustrating the macroscopic response decay with respect to time of agonist exposure; wild-type in black,  $\alpha 4S336A$  in red, and  $\alpha 4S336D$  in blue. **(c)** Bar graphs showing the average percentage of current lost after repetitive applications of agonist. **(d)** Percent recovery of the original macroscopic response after 20 min of agonist withdrawal for wild-type,  $\alpha 4S336A$ , and  $\alpha 4S336D$   $\alpha 4\beta 2$  nAChRs. Statistical analyses were performed using one-way ANOVA with Dunnett's multiple comparison test ( $P < 0.05$ ;  $** P < 0.01$ ;  $*** P < 0.001$ ). Data were obtained from 7 to 29 oocytes

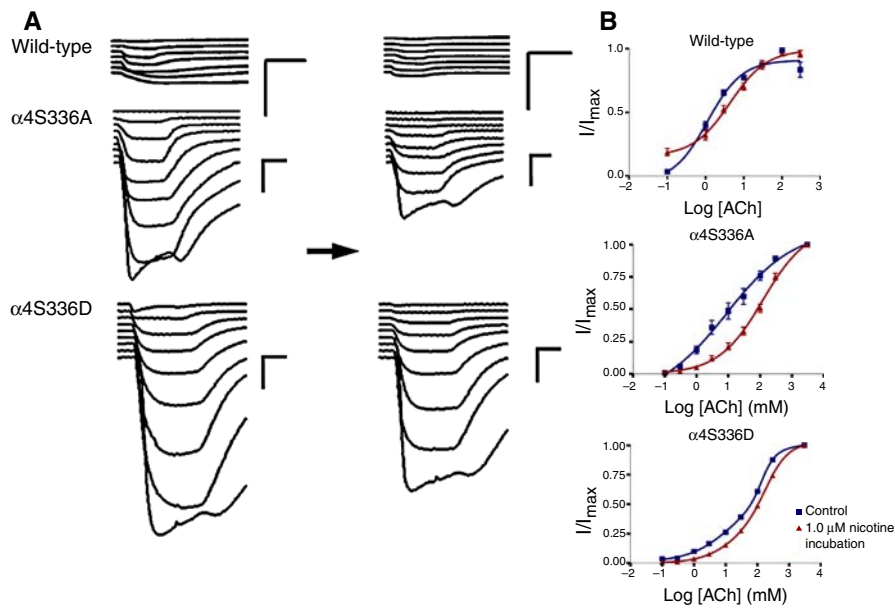


**Fig. 3** Effect of chronic nicotine exposure on the ACh-induced response of  $\alpha 4S336$  mutants expressed in *Xenopus* oocytes. Voltage clamp recording was used to determine the ACh-induced response of *Xenopus* oocytes expressing wild-type,  $\alpha 4S336A$ , and  $\alpha 4S336D$  nAChRs before and after chronic nicotine exposure. **(Left side)** shows the family of currents for the control experiments (without chronic nicotine incubation), whereas **(right side)** illustrates the currents after chronic nicotine exposure. **Horizontal black arrow** represents 24 h of 1.0  $\mu M$  nicotine incubation. After chronic nicotine treatment and prior to voltage clamp recording, oocytes were washed for 6 min perfusing with MOR2 buffer. Calibration bars are shown at the **right** of each current family, 500 nA (vertical bars) and 8 s (horizontal bars). **(b)** ACh dose–response curves for wild-type,  $\alpha 4S336A$ , and  $\alpha 4S336D$  nAChRs, before and after chronic nicotine treatment. Dose–response relationships were determined using nine ACh concentrations for  $\alpha 4S336A$  and  $\alpha 4S336D$  mutants (0.1, 0.3, 1, 3, 10, 30, 100, 300, and 3,000 nM) and seven doses for wild-type nAChR (0.1, 1, 3, 10, 30, 100, and 300 nM). ACh-induced currents were normalized to the maximum response ( $I/I_{max}$ ). A better curve fit was obtained using the two-component Hill equation for  $\alpha 4S336D$  mutant. Data from control oocytes are shown in **blue**, whereas the results after 24 h of 1.0  $\mu M$  nicotine incubation are shown in **red**. Dose–response curves represent the average and standard error of the mean for 5–9 oocytes

expressing mutant or wild-type nAChRs, their responses to several concentrations of ACh were measured after 24 h incubation in 1  $\mu M$  nicotine (Fig. 3a, right traces). After chronic nicotine treatment the mutants and wild-type nAChRs exhibited a reduced state of activation as evidenced by a significant decrease in their respective peak currents (Table 2). Furthermore, after chronic nicotine exposure all three nAChR subtypes displayed a significant increase in the  $E_{50}$  values for ACh (Fig. 3 and Table 2), whereas there was no significant difference in the Hill coefficient values. The  $\alpha 4S336A$  mutant exhibited a dramatic inactivation evidenced by a 15-fold shift in the  $E_{50}$  value for ACh. In the case of the  $\alpha 4S336D$  mutant only the component of lower ACh sensitivity showed a

significant increase in the  $E_{50}$  value for ACh after chronic nicotine exposure (Table 2).

#### Up-regulation of $\alpha 4\beta 2$ nAChRs

Whole-mount immunofluorescence assays for the detection of surface  $\alpha 4$  subunit and confocal imaging were performed to determine the effects of chronic nicotine exposure on the up-regulation of mutant  $\alpha 4\beta 2$  nAChRs. Oocytes were paired according to their similar current profile (i.e., not more than 400 nA difference); oocytes incubated for 24 h with 1.0  $\mu M$  nicotine were compared with oocytes without nicotine exposure. Figure 4 illustrates representative confocal sections of immunolabeled  $\alpha 4$  subunit on the surface membranes of *Xenopus* oocytes and their

Table 2 Effects of chronic nicotine exposure in the functional properties of  $\alpha 4\beta 2$  mutants

	Wild-type	$\alpha 4S336A$	$\alpha 4S336D$	
Peak current at 300 $\mu M$ ACh (nA $\pm$ SE)				
Control	479 $\pm$ 86	1,790 $\pm$ 280	1,684 $\pm$ 176	
1 $\mu M$ nicotine incubation	246 $\pm$ 60* (n = 19)	1,128 $\pm$ 251* (n = 22)	1,257 $\pm$ 163* (n = 21)	
EC <sub>50</sub> ACh ( $\mu M$ $\pm$ SE)				
Control	1.1 $\pm$ 0.1	8.6 $\pm$ 0.2	17.4 $\pm$ 1.4	137.7 $\pm$ 0.1
1 $\mu M$ nicotine incubation	4.38 $\pm$ 0.1* (n = 9)	124.7 $\pm$ 0.1* (n = 9)	18.2 $\pm$ 1.4 (n = 5)	194.1 $\pm$ 0.2*
Hill slope ACh				
Control	0.97 $\pm$ 0.1	0.4 $\pm$ 0.1	0.6 $\pm$ 0.4	2.2 $\pm$ 2.7
1 $\mu M$ nicotine incubation	0.9 $\pm$ 0.1 (n = 9)	0.6 $\pm$ 0.1 (n = 9)	0.8 $\pm$ 0.4 (n = 5)	1.2 $\pm$ 0.4

Values are given as the mean  $\pm$  SEM. \* Indicates  $P < 0.05$ ,  $n$  indicates the number of oocytes tested, 300  $\mu M$  ACh and 30  $\mu M$  nicotine were used to estimate the peak currents

corresponding fluorescence intensity profiles for each  $\alpha 4\beta 2$  subtype studied. The total fluorescence intensity for each confocal section was calculated as explained under section "Materials and methods." Figure 4b shows a plot of the average fold values (intensity after chronic nicotine exposure divided by the intensity before chronic nicotine exposure) for each  $\alpha 4\beta 2$  subtype. The average fold values were  $1.1 \pm 0.1$  and  $1.1 \pm 0.1$  for the  $\alpha 4S336A$  and  $\alpha 4S336D$  mutants, respectively. In contrast, the average fold value for the wild-type  $\alpha 4\beta 2$  receptor was  $2.0 \pm 0.2$  evidenced by the increment in the fluorescence intensity observed in oocytes expressing wild-type  $\alpha 4\beta 2$  nAChRs that were exposed to chronic nicotine incubation (Fig. 4a). The average fold values were significantly different between both mutants and wild-type  $\alpha 4\beta 2$  nAChRs ( $P = 0.0069$ ).

## Discussion

Neuronal nAChR subunits are subject to phosphorylation by cyclic AMP-dependent PKA and PKC. Such chemical modifications may regulate agonist-induced desensitization (Downing and Role, 1987; Vijayaraghavan et al. 1990). Activation of protein kinases, such as PKA and PKC, has been demonstrated to promote recovery from desensitization by an increase in the fraction of functional receptors (Fenster et al. 1999a; Khiroug et al. 1998). The  $\alpha 4$  subunit contains at least nine serine phosphorylation consensus sites. Several in vitro studies have

demonstrated that some of these sites are directly phosphorylated by PKA or PKC (Moss et al. 1996; Nakayama et al. 1993; Vijayaraghavan et al. 1990; Wecker et al. 2001). In the present study, one of the putative phosphorylation consensus sites in the nAChR subunit, S336, has been replaced with either alanine or aspartic acid. The alanine substitution removed the potential phosphorylation consensus site and aspartic acid was used to mimic the negative charge at position  $\alpha 4S336$ . We used both ACh and nicotine as agonists to determine the effect of these mutations on the activation, desensitization, and nicotine-induced up-regulation of  $\alpha 4\beta 2$  nAChRs expressed in *Xenopus* oocytes. The results presented here demonstrate the contribution of the  $\alpha 4S336$  residue to the functional regulation of  $\alpha 4\beta 2$  nAChRs expressed in *Xenopus* oocytes.

## Functional Implications

The electrophysiological data revealed differences, both in macroscopic peak current and in activation properties, between mutant and wild-type  $\alpha 4\beta 2$  nAChRs when using ACh as agonist (Fig. 1 and Table 1). Mutant receptors exhibited a threefold increase in the ACh-induced macroscopic current. The observed increment in macroscopic current could be caused by an increase in the fraction of functional receptors assembled in the plasma membrane of oocytes or a large unitary conductance compared to the wild-type receptor. Epibatidine binding confirmed that, when

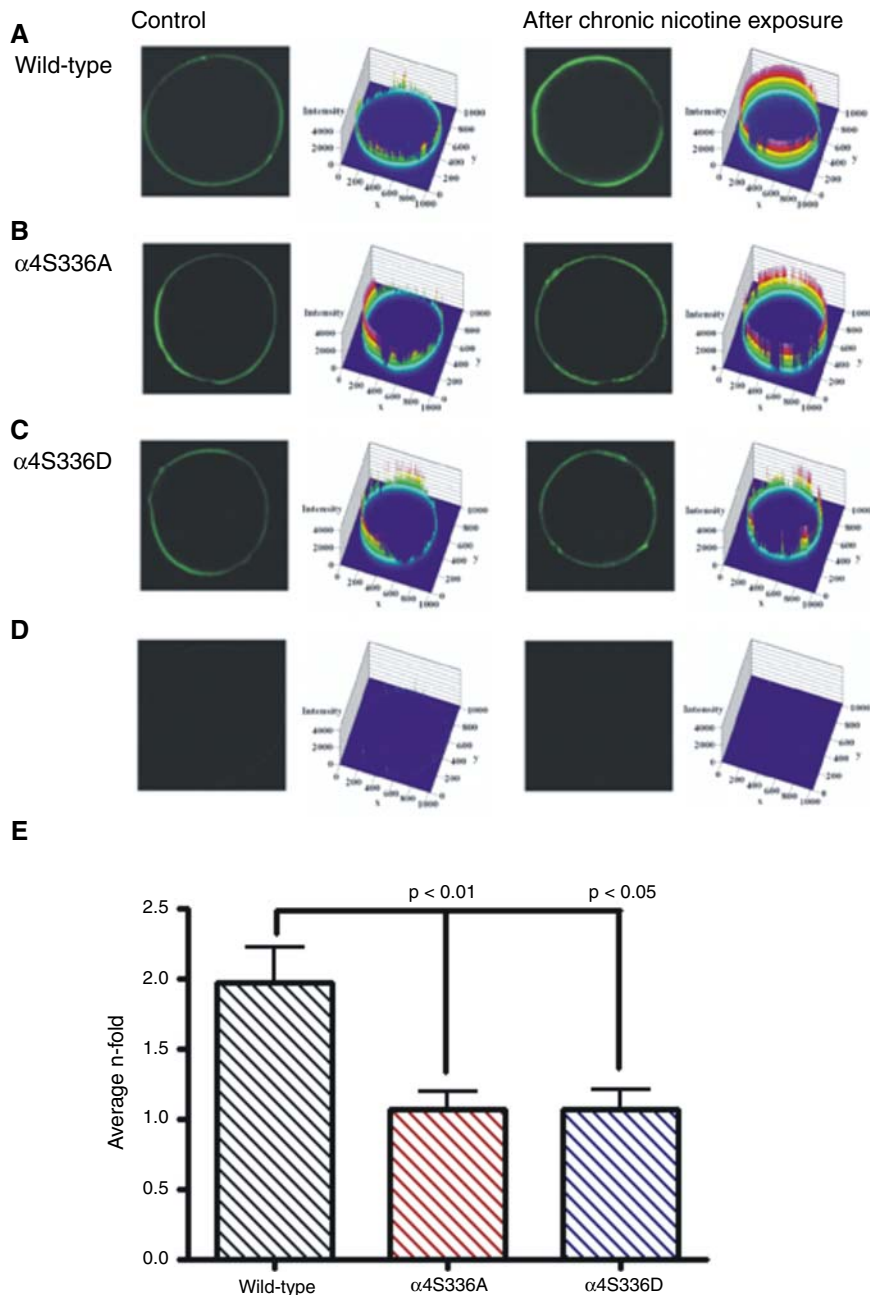


**Fig. 4** Confocal images of the immunofluorescence surface detection of the  $\alpha 4$  subunit after chronic nicotine exposure (a) Fluorescence intensity of oocytes injected with wild-type  $\alpha 4$ . The initial response at 300  $\mu M$  ACh for the incubated oocyte was 3,333 and 2,834 nA for the control oocyte (b) Fluorescence intensity of oocytes injected with  $\alpha 4S336A$  mutant. The initial responses at 300  $\mu M$  ACh for the incubated and control oocytes were 1,968 and 1,704 nA, respectively (c) Fluorescence

intensity of oocytes injected with  $\alpha 4S336D$  mutant. The initial response at 300  $\mu M$  ACh for the incubated oocyte was 1,830 and 1,876 nA for the control oocyte (d) Fluorescence intensity of oocyte not injected but treated with primary and secondary antibodies (left). Oocyte injected with wild-type  $\alpha 4b2$  (335 nA) but treated with primary antibody (right). (e) The average n-fold values are presented as bar graphs for wild-type (black),  $\alpha 4S336A$  (red), and  $\alpha 4S336D$  (blue)

compared to wild-type, both mutations result in an increase in the number of  $\alpha 4\beta 2$  receptors in the oocyte membrane (Fig. 1d). Both mutations displayed a significant increase in the  $EC_{50}$  value for ACh (Fig. 1 and Table 1). However, the dose–response curve generated for the  $\alpha 4S336D$  mutant was best fitted using a two-component Hill equation, whereas the  $\alpha 4S336A$  mutation results in a less sigmoidal dose–response curve (Fig. 1b). These observations suggest that elimination of the serine consensus site has different dynamic and/or structural requirements results in a less allosteric nAChR, while addition of a negative charge in the S336 residue, as with the  $\alpha 4S336D$  mutation, results in a more allosteric nAChR. The present data suggest that residue S336 plays a crucial role in the functional state of the  $\alpha 4\beta 2$  receptor.

It is noteworthy that, even though the mutants showed distinct activation properties induced by ACh, the  $EC_{50}$  and Hill coefficient values for nicotine activation and the nicotine-induced macroscopic peak current remained unaffected (Fig. 1 and Table 1). Consistent with our previous study (López-Hernández et al. 2004), the marked differences between ACh and nicotine effects seen in the data presented here suggest that the properties of agonist binding for  $\alpha 4\beta 2$  channel activation have very distinct dynamic and/or structural requirements for ACh and nicotine.

#### Desensitization and Nicotine-induced Up-regulation

Following repetitive applications of ACh, the  $\alpha 4S336D$  mutant displayed more resistance to ACh-induced desensitization (Fig. 2a–c), as evidenced by its lowest percent current loss, when compared to wild-type and  $\alpha 4S336A$ . The agonist-induced desensitization was more evident when consecutive pulses of nicotine were applied to the oocytes expressing mutant or wild-type  $\alpha 4\beta 2$  receptors (Fig. 2a–c). The  $\alpha 4S336A$  mutant displayed the largest nicotine-induced desensitization, whereas the  $\alpha 4S336D$  mutant showed no significant difference, compared to wild-type, in the percent current loss following consecutive applications of  $30 \mu M$  nicotine (Fig. 2a–c). Compared to wild-type  $\alpha 4\beta 2$  nAChR, both mutants exhibited a significant decrease in the percent current recovered after nicotine-induced desensitization. Specifically,  $\alpha 4S336A$  and  $\alpha 4S336D$  mutants recovered <40% of their original macroscopic current following

consecutive applications of  $30 \mu M$  nicotine (Fig. 2d). It is noteworthy that although the mutants did not differ from wild-type in the activation properties induced by nicotine (Fig. 1c), there were changes with respect to the percentage of current lost and in the recovery from desensitization after consecutive nicotine applications. This supports our previous hypothesis, which proposes that the site responsible for nicotine-induced activation of the  $\alpha 4\beta 2$  nAChR has different dynamic and/or structural requirements from the site that promotes channel desensitization (López-Hernández et al. 2004).

Both mutants exhibited different patterns of functional regulation, in control condition as well as after chronic nicotine exposure. For example, the ACh dose–response curve for the  $\alpha 4S336D$  mutant was best fitted using a two-component Hill equation, whereas the  $\alpha 4S336A$  mutant and the wild-type receptor were fitted using a single Hill equation. Moreover, dose–response relationships obtained from chronic nicotine exposure experiments revealed differences in the allosteric transitions of the receptor between wild-type and both  $\alpha 4S336$  mutants. That is, the  $\alpha 4S336A$  mutant appears to be a less allosteric receptor before chronic nicotine exposure (Fig. 1b). The latter finding may account for the dramatic inactivation observed in this mutant after chronic nicotine exposure, i.e., a 14-fold increase in  $EC_{50}$  after chronic nicotine incubation (Table 2). Alternatively, the two component Hill equation fit for the  $\alpha 4S336D$  data might suggest that this mutation results in two distinct populations of nAChRs in the membrane, one with high sensitivity to ACh ( $EC_{50} = 17.4 \mu M$ ; Table 2) and the other with lower sensitivity to ACh ( $EC_{50} = 137.7 \mu M$ ; Table 2). Overall, these results demonstrated that the PKC consensus  $\alpha 4S336$  position might play a remarkable role in the allosteric properties of the  $\alpha 4\beta 2$  nAChR.

Both S336 mutants failed to display a significant up-regulation after chronic nicotine exposure. This finding could be explained by the fact that both mutants display a remarkable enhance on the expression of the  $\alpha 4\beta 2$  nAChR, therefore, it seems that chronic nicotine exposure cannot up-regulate a receptor that is already over expressed compared to wild-type. Based on these results, we hypothesize that phosphorylation at multiple consensus sites in this domain induces a conformational change that triggers an intracellular signal responsible for the desensitization of  $\alpha 4\beta 2$

nAChRs and consequently the nicotine-induced up-regulation process. However, the present data suggest that adding or removing a negative charge at this phosphorylation site cannot be explained by a simple straightforward on-and-off mechanism; rather a more complex mechanism(s) may govern the functional expression of the  $\alpha 4\beta 2$  nAChR. Along the same line, our data support the idea that phosphorylation at multiple consensus sites in the  $\beta 2$  subunit has a critical role on the regulation of the functional expression of the  $\alpha 4\beta 2$  nAChR. One appealing hypothesis is that phosphorylation at multiple consensus sites in the  $\beta 2$  subunit might lead to receptors with altered stoichiometry. For instance, the activation profile of the  $\alpha 4S336D$  mutation is very similar to the parameters of the  $\alpha 4(4)1(\beta 2)$  nAChR reported in our previous study (López-Hernández et al 2004).

Finally, our results indicate the importance of the  $\alpha 4S336$  residue in the functional regulation of the  $\alpha 4\beta 2$  nAChR. The  $\alpha 4S336$  position could provide a way to re-tune synaptic transmission of  $\alpha 4\beta 2$  receptors and could be of great physiological relevance given the critical role of neuronal nAChRs in presynaptic membranes where they modify the excitability of neurons and facilitate neurotransmitter release.

**Acknowledgments** We thank Mr. José Serrano, Dr. Janice Salas, and Dr. Amelia Rivera for valuable technical assistance. This research was supported by National Institutes of Health Grants NIH 2R01GM56371-11, SNRP-U54NS4301, and GM08102-27. The Research Initiative for Scientific Enhancement-Minority Biomedical Research Support (RISE-MBRS)-NIH program (5R25GM61151) supported Gretchen Y. López-Hernández. Nilza M. Biaggi-Labiosa was supported by the RISE-MBRS-NIH program (2R25GM061151). Alexis Torres-Cintrón was supported by the Minority Access to Research Careers (MARC)-MBRS-NIH program.

## References

- Benwell ME, Balfour DJ, Anderson JM (1988) Evidence that tobacco smoking increases the density of [ $^3$ H]nicotine binding sites in human brain. *J Neurochem* 50:1243–1247. doi:10.1111/j.1471-4159.1988.tb10600.x
- Breese CR, Marks MJ, Logel J, Adams CE, Sullivan B, Collins AC et al (1997) Effect of smoking history on [ $^3$ H]nicotine binding in human postmortem brain. *J Pharmacol Exp Ther* 282:7–13
- Downing JE, Role L (1987) Activators of protein kinase C enhance acetylcholine receptor desensitization in sympathetic ganglion neurons. *Proc Natl Acad Sci USA* 84:7739–7743. doi:10.1073/pnas.84.21.7739
- Eilers H, Schaeffer E, Bickler PE, Forsayeth JR (1997) Functional deactivation of the major neuronal nicotinic receptor caused by nicotine and a protein kinase C-dependent mechanism. *Mol Pharmacol* 52:1105–1112
- Fenster CP, Beckman ML, Parker JC, Shefeld EB, Whitworth TL, Quick MW et al (1999a) Regulation of  $\alpha 4\beta 2$  nicotinic receptor desensitization by calcium and protein kinase C. *Mol Pharmacol* 55:432–443
- Fenster CP, Whitworth TL, Shefeld EB, Quick MW, Lester RA (1999b) Upregulation of surface  $\alpha 4\beta 2$  nicotinic receptors is initiated by receptor desensitization after chronic exposure to nicotine. *J Neurosci* 19:4804–4814
- Flores CM, Rogers SW, Pabreza LA, Wolfe BB, Kellar KJ (1992) A subtype of nicotinic cholinergic receptor in rat brain is composed of  $\alpha 4$  and  $\beta 2$  subunits and is up-regulated by chronic nicotine treatment. *Mol Pharmacol* 41:31–37
- Huganir RL, Delcour AH, Greengard P, Hess GP (1986) Phosphorylation of the nicotinic acetylcholine receptor regulates its rate of desensitization. *Nature* 321:774–776. doi:10.1038/321774a0
- Ke L, Eisenhour CM, Bencherif M, Lukas RJ (1998) Effects of chronic nicotine treatment on expression of diverse nicotinic acetylcholine receptor subtypes I. Dose- and time-dependent effects of nicotine treatment. *J Pharmacol Exp Ther* 286:825–840
- Khiroug L, Sokolova E, Giniatullin R, Afzalov R, Nistri A (1998) Recovery from desensitization of neuronal nicotinic acetylcholine receptors of rat chromaffin cells is modulated by intracellular calcium through distinct second messengers. *J Neurosci* 18:2458–2466
- Lapchack PA, Araujo DM, Quirion R, Collier B (1989) Effect of chronic nicotine treatment on nicotinic autoreceptor function and N-3H-Mcc binding sites in the rat brain. *J Neurochem* 52:483–491. doi:10.1111/j.1471-4159.1989.tb09146.x
- López-Hernández GY, Sánchez-Padilla J, Ortiz-Acevedo A, Lizardi-Ortiz J, Salas-Vincenty J, Rojas V et al (2004) Nicotine-induced up-regulation and desensitization of neuronal nicotinic receptors depend on subunit ratio. *J Biol Chem* 279:38007–38015. doi:10.1074/jbc.M403537200
- Lukas RJ (1991) Effects of chronic nicotinic ligand exposure on functional activity of nicotinic acetylcholine receptors expressed by cells of the PC12 rat pheochromocytoma or the TE671/RD human clonal line. *J Neurochem* 56:1134–1145. doi:10.1111/j.1471-4159.1991.tb11403.x
- Marks MJ, Burch JB, Collins AC (1983) Effects of chronic nicotine infusion on tolerance development and nicotinic receptors. *J Pharmacol Exp Ther* 226:817–825
- Moss SJ, McDonald BJ, Rudhard Y, Schoepfer R (1996) Phosphorylation of the predicted major intracellular domains of the rat and chick neuronal nicotinic acetylcholine receptor  $\alpha 7$  subunit by cAMP-dependent protein kinase. *Neuropharmacology* 35:1023–1028. doi:10.1016/S0028-3908(96)00083-4
- Nakayama H, Okuda H, Nakashima T (1993) Phosphorylation of rat brain nicotinic acetylcholine receptor by cAMP-dependent protein kinase in vitro. *Brain Res Mol Brain Res* 20:171–177. doi:10.1016/0169-328X(93)90123-7
- Schwartz RD, Kellar KJ (1985) In vivo regulation of [ $^3$ H]acetylcholine recognition sites in brain by nicotinic

- cholinergic drugs. *J Neurochem* 45:427–433. doi:10.1111/j.1471-4159.1985.tb04005.x
- Swope SL, Moss SJ, Blackstone CD, Hagan RL (1992) Phosphorylation of ligand-gated ion channels: a possible mode of synaptic plasticity. *FASEB* 6:2514–2523
- Vijayaraghavan S, Schmid HA, Halvorsen SW, Berg DK (1990) Cyclic AMP-dependent phosphorylation of a neuronal acetylcholine receptor alpha-type subunit. *J Neurosci* 10:3255–3262
- Viseshakul N, Figl A, Lytle C, Cohen BN (1998) The alpha4 subunit of rat alpha4beta2 nicotinic receptors is phosphorylated in vivo. *Brain Res Mol Brain Res* 59:100–104. doi:10.1016/S0169-328X(98)00128-4
- Wecker L, Guo X, Rycerz AM, Edwards SC (2001) Cyclic AMP-dependent protein kinase (PKA) and protein kinase C phosphorylate sites in the amino acid sequence corresponding to the M3/M4 cytoplasmic domain of alpha4 neuronal nicotinic receptor subunits. *J Neurochem* 76:711–720. doi:10.1046/j.1471-4159.2001.00041.x
- Whiteaker P, Sharples CG, Wonnacott S (1998) Agonist-induced up-regulation of alpha4beta2 nicotinic acetylcholine receptors in M10 cells: pharmacological and spatial de nition. *Mol Pharmacol* 53:950–962